Lift Augmentation for Vertical Axis Wind Turbines

Gerald M. Angle II gerald.angle@mail.wvu.edu
Post Doctoral Fellow/Department of Mechanical and
Aerospace Engineering/Center for Industrial Research Applications
West Virginia University
Morgantown, WV 26506-6106, USA

Franz A. Pertl franz.pertl@mail.wvu.edu
Program Coordinator/Department of Mechanical and
Aerospace Engineering/Center for Industrial Research Applications
West Virginia University
Morgantown, WV 26506-6106, USA

Mary Ann Clarke maclarke@math.wvu.edu
Assistant Professor/Department of Mathematics
West Virginia University
Morgantown, WV 26506-6310, USA

James E. Smith james.smith@mail.wvu.edu
Professor and Director/Department of Mechanical and
Aerospace Engineering/Center for Industrial Research Applications
West Virginia University
Morgantown, WV 26506-6106, USA

Abstract

The concept of harnessing wind power has been around for centuries, and is first recorded by the Persians in 900 AD. These early uses of wind power were for the processing of food, particularly grinding grains, and consisted of stationary blades around a horizontal axis, the precursor to today's horizontal axis wind turbines (HAWT). Technology for these wind mills was essentially the same until the 1930's when advances in aircraft propeller theories were applied to the blades of the turbine. During this development period, which has since remained basically unchanged, the design push was for increasingly larger propellers requiring heavy and costly transmissions, generators, and support towers to be installed.

An alternative concept to the HAWT was developed by Georges Darrieus [1], which utilized a vertical shaft and is known as a vertical axis wind turbine (VAWT). The scientific development of the concept did not gain strong attention until the 1970's due to the perceived low efficiency of this style. This perception was due in part to the portion of the blade's rotary path that is adverse to the generation of power. This efficiency loss can be minimized by the mechanical movement of the blade, relative to the airflow during the upwind portion of the blades' rotational path. Since, circulation control can alter the forces generated by an airfoil, it could be used to increase the efficiency of a VAWT by increasing

the torque produced on the downwind portion of the path, while removing the need for a physical change in angle of attack.

With the recent upturn in petroleum costs and global warming concerns, interest in renewable energy technologies have been reinvigorated, in particular the desire for advanced wind energy technologies, including the application of lift augmentation techniques. One of these techniques is to utilize circulation control to enhance the lifting capacity of the blades based on the location of the blade in the turbine's rotation. Though this technology can be applied to any wind turbine, whether horizontal or vertical axis, this paper focuses on the application of circulation control for VAWT's due primarily to reduced hardware complexities and to increase the performance of this design thus helping to level the playing field between the two styles. This performance enhancement coupled with the ability to locate the primary components near the ground allows for easier installation, troubleshooting, maintenance, and future improvement of the circulation control sub-system.

By varying the circulation control performance with the blade position, the coefficient of performance, C_p, of the wind turbine can be altered. This variation in C_p resembles a change in the effective solidity factor, the non-dimensional characteristic that accounts for the number of turbine blades, chord length, and turbine radius. The solidity factor is typically used in the design of a wind turbine with its peak performance occurring at various tip speed ratios, at different solidity factors.

Prior to the construction of physical models, numerical methods, namely a vortex model, was used to estimate the performance enhancement potential of the blade force augmentation via circulation control. These results were then used to construct and test a wind tunnel blade section model to obtain lift and drag values for a full range of rotational angles. These results were then supplied to the vortex model which indicated that through the addition of circulation control to the blades of a vertical axis wind turbine a wider coefficient of performance curve can be achieved, similar to a change in the solidity factor of the wind turbine.

Keywords: Circulation Control, Vertical Axis Wind Turbine, Vortex Model.

1. INTRODUCTION

The maximum power extractable from wind at a specified velocity flowing through a turbine area, A, is defined by the Betz limit, 16/27. This limit has been derived by considering the momentum loss between the upstream and downstream velocities, V_1 and V_2, respectively, as shown in Eq. (1).

$$P = \frac{1}{2}\rho A\left(\frac{V_1+V_2}{2}\right)\left(V_1^2 - V_2^2\right) \quad (1)$$

The maximum extractable power of ~59% of the available power occurs when V_2 (downstream) is approximately one third of V_1 (upstream). Substituting the free stream velocity, V_∞, into Eq. (1), results in Eq. (2) for the maximum power extractable from a wind according to the Betz limit, relative to the overall power available in the wind. The coefficient of performance, C_p, defined in Eq. (3), is a representation of the ratio of actual power produced-to-maximum power available in the wind.

$$P_{\max} = \frac{16}{27}\left(\frac{1}{2}\right)\rho A V_\infty^{\,3} \tag{2}$$

$$C_p = \frac{\left(1+\frac{V_2}{V_1}\right)\left[1-\left(\frac{V_2}{V_1}\right)^2\right]}{2} \tag{3}$$

The theoretical maximum coefficient of performance, 16/27, is never achieved by practical wind turbines due to the irregularities in the wind speed and other environmental factors. A more realistic value for the C_p for existing wind turbines range from 30-50%, or 51-85% of the Betz limit. Thus, the power extracted by a wind turbine can be defined based on an efficiency, η, density, ρ, the turbine's capture area and the wind velocity as is shown in Eq. (4). This definition of efficiency is with respect to the Betz limit, thus if the coefficient of performance is 0.45, the efficiency is 76%. The power produced depends on the wind-speed cubed, thus it is important to know the wind speed of the intended site in order to predict the power capacity of a wind turbine. This study is based on the H-Shaped Darrieus Vertical Axis Wind Turbine as previously investigated by Kuhlke [2], Migliore [3], and Migliore et al. [4].

$$P_\eta = \eta\frac{16}{27}\left(\frac{1}{2}\right)\rho S V_\infty^{\,3} \tag{4}$$

2. IMPLEMENTED VORTEX MODEL

The approach taken to evaluate the performance of the VAWT was to use the vortex model by combining the Kutta-Joukowski law, Eq. (5), with the aerodynamic lift force exerted by the blade per unit span, Eq. (6). By equating these two relationships, the influence of the lift force on the air surrounding the VAWT, can be investigated using Eq. (7).

$$L' = \rho V \Gamma \tag{5}$$

$$L' = \frac{1}{2}\rho V^2 c C_\ell \tag{6}$$

$$\Gamma = \frac{1}{2} V c C_\ell \tag{7}$$

However, the aerodynamic forces change with angle-of-attack, thus the circulation created by the wind turbine blade is also dependent on the angle-of-attack, and consequently dependent upon the rotational location of the turbine blade with respect to the direction of the wind plus the tip speed ratio. The vortex model incorporates a time dependent analysis, taking small time steps to analyze the wind turbine performance. Each blade has an associated "bound vortex", Γ_B, with a strength based on the lift force of the current conditions (angle-of-attack, speed, etc) which moves with the blade, around the turbine. As the strength of the bound vortex changes from time step, *NT*, to time step, *NT-1*, the difference between the vortex strength defines the strength of the vortex that is shed, Γ_S, as is illustrated in FIGURE 1 and defined in Eq.(8).

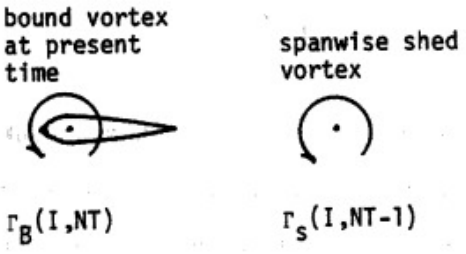

FIGURE 1: Diagram of the Spanwise Shed Vortex, Strickland, et al. [5].

$$\Gamma_s(i, NT-1) = \Gamma_B(i, NT-1) - \Gamma_B(i, NT) \tag{8}$$

The induced velocity at a point (i, j) in the flow, due to a single vortex can be found using Eq.(9). In complex flows, such as for the VAWT, the induced velocity is determined based on the sum of all the vortex strengths, bound and shed, in the spanwise direction and is due to the lift generation, i.e. trailing vortices, as shown in Eq. (10).

$$\vec{V}_p = \frac{\Gamma}{4\pi}\int_{\ell}\frac{\vec{r}\times d\vec{\ell}}{r^3} \tag{9}$$

$$\vec{V}(i,j) = \sum_{k=1}^{NE}\sum_{\ell=1}^{NT-1}\vec{V}_p\Big|_{trailing\ \ vortices} + \sum_{k=1}^{NE-1}\sum_{\ell=1}^{NT}\vec{V}_p\Big|_{spanwise\ \ vortices} \tag{10}$$

After prediction of the induced velocities, the bound vortex strength was updated using Eq. (7) along with the new velocities, which were then used to update the induced velocity using Eq. (9). Note that this relationship is only valid outside of a given radius, “core” of the vortex. The velocity at the edge of the vortex core, V_c, if found using Eq. (11), the corresponding radius, h_c, is defined by Eq. (12). FIGURE 2 illustrates the velocity profile in the vicinity of a vortex, where a zero velocity is imposed at the core center and a linear profile is applied to the calculated velocity at the edge of the core. Strickland, et al. [5] notes that the core velocity is independent of the $\Delta\theta$ angle when the step is reasonably small; however, the core radius is proportional to the angular increment. Eq. (13) was used to represent the velocity near the core as a single function, as done by Pawsey [6], rather than the piecewise function of Strickland, et al. [5], resulting in the profile shown in FIGURE 3.

$$V_c = \frac{1}{2}\frac{\Gamma}{R(\Delta\theta)} \tag{11}$$

$$h_c = \frac{R(\Delta\theta)}{\pi} \tag{12}$$

$$V_c = \frac{\Gamma h}{2\pi\left(h^2 + \left(\frac{R\,\omega\Delta t}{2\pi}\right)^2\right)} \tag{13}$$

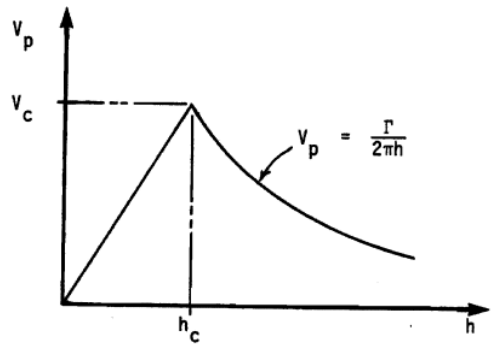

FIGURE 2: Velocity Profile of Vortex with Viscous Core, Strickland, et al. [5]**.**

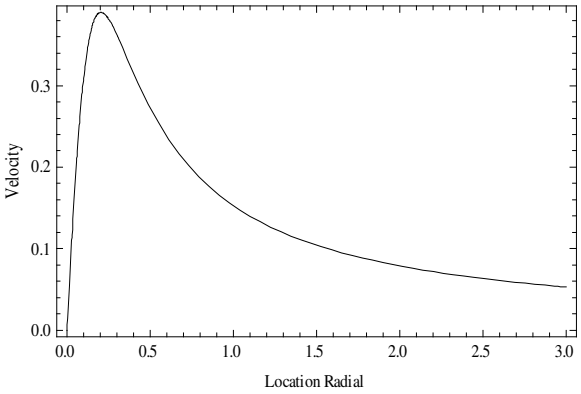

FIGURE 3: Representation of the Velocity Profile with $R = 1$ using Eq. 13 from Pawsey [6].

A vortex is shed from the blade at every time step in the analysis, and is transmitted downstream by the induced velocity due to all vortices in the flow field. The shed vortices are transmitted downstream until they exit the analytical space, generally five rotor diameters downstream, which allows for the visualization of multiple revolutions of the wind turbine.

As the resultant velocity, U_R, is determined, the tangential force per unit length, F_t', acting in the direction of motion and the normal force per unit length, F_n', can be determined using Eqs. (14) and (15), respectively. The non-dimensional version of these relationships, F_t^+ and F_n^+, Eqs. (16) and (17), are non-dimensionalized with respect to the freestream velocity, U_∞.

$$F_t' = \frac{1}{2} C_t \rho c U_R^2 \tag{14}$$

$$F_n' = \frac{1}{2} C_n \rho c U_R^2 \tag{15}$$

$$F_t^+ = \frac{F_t'}{\frac{1}{2}\rho c U_\infty^2} = C_t \left(\frac{U_R}{U_\infty} \right)^2 \tag{16}$$

$$F_n^+ = \frac{F_n'}{\frac{1}{2}\rho c U_\infty^2} = C_n \left(\frac{U_R}{U_\infty} \right)^2 \tag{17}$$

Eq. (18) defines the torque produced by one element (blade) based on the tangential force per unit length, as well as its non-dimensional form. The power coefficient (coefficient of performance) at each time step is determined by Eq. (19) for an individual blade. To obtain the coefficient of performance for the entire rotor the average value for a complete revolution is found from Eq. (20), based on the number of time increments, *NTI*, and the number of elements, *NE*, (blades).

$$T_e^+ = \frac{F_t'}{RU_\infty^2} = \frac{1}{2}\left(\frac{c}{R}\right)F_t^+ \tag{18}$$

$$C_{p_{element}} = T_e^+ \frac{U_T}{U_\infty} \tag{19}$$

$$C_p = \frac{1}{NTI}\sum_{1}^{NTI}\sum_{1}^{NE-1} C_{p_{element}} \tag{20}$$

The coefficient of performance is dependent on the solidity factor, σ, as well as the tip speed ratio, λ, as shown in FIGURE 4 for an unaltered NACA 0012 blade cross-sectional shape. As the solidity factor is increased the low tip speed ratio performance in increased, where a maximum Cp of approximately 0.42 is achieved at solidity factors of 0.2 and 0.4. However, at low tip speed ratios the peak coefficient of performance is decreased while an increasing coefficient of performance can be achieved at higher tip speeds. For example, a solidity of 0.1 reaches a Cp of zero at a tip speed of 10.5, whereas a solidity of 0.2 reaches zero at just over a tip speed ratio of 8. FIGURE 4 represents a series of plots for solidity factors, σ, from 0.0125 to 0.8 over the range of tip speed ratios, λ, up to 12. These curves represent the potential power capture ratios for a given solidity factor wind turbine, where the designer would select the single curve that would result in the greatest energy capture for the given wind conditions of the intended site.

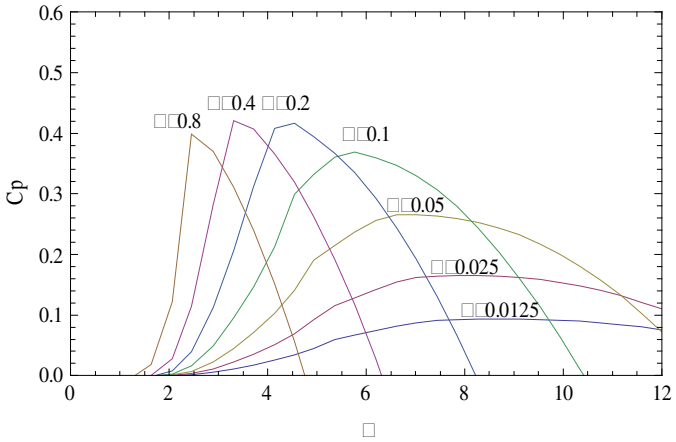

FIGURE 4: Coefficient of Performance using a NACA0012 Airfoil at Re = 300,000, for various σ Values, McGrain, et al. [7]**.**

3. APPLICATION BACKGROUND OF CIRCULATION CONTROL

The initial research and later applications of circulation control technologies were for short take-off, fixed-wing aircraft which were initially built and tested in the late 1960's and 1970's. This phenomenon re-energizes the boundary layer near the trailing edge, as shown in FIGURE 5, of an airfoil with a rounded trailing edge which enhances the circulation around the wing. Introducing a blowing jet tangent to the surface, either inclined or rounded, creates a pressure force deflecting the jet towards the surface, as introduced by Newman [8]. For a rounded surface, such as a cylinder as investigated by Churchill [9], or a modified trailing edge of an airfoil as studied by

Ambrosiani [10], Englar [11], Kind [12], Kind and Maull [13], and Myer [14], to name a few of the many investigators, this pressure force overcomes the centrifugal (inertial) force of the jet. As the jet flow travels along the surface, the pressure force decreases until the inertial force is greater, at which point flow separates from the surface.

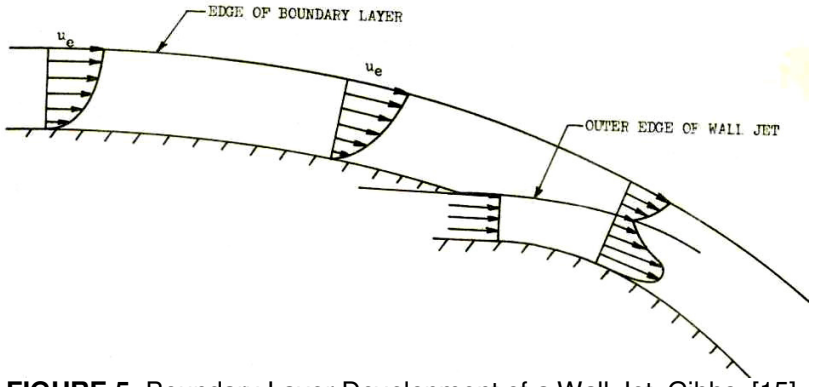

FIGURE 5: Boundary Layer Development of a Wall Jet, Gibbs, [15].

The blown jet in turn entrains the freestream airflow, effectively altering the interaction of the airfoil with the surrounding fluid. This change in effective shape alters the lift and drag performance of the airfoil. The amount of change in the aerodynamic forces is a function of the blowing coefficient which is a non-dimensional ratio of jet momentum to the freestream momentum. The blowing coefficient, C_μ, is a function of the density, ρ, velocity, V, of the jet and free-stream as prescribed by the subscripts j and ∞, respectively, and slot height, h, chord length, c, and the span of the jet and turbine blade, b_j and b_s, respectively, as is shown in Eq. (21).

$$C_\mu = \frac{\rho_j V_j^2 b_j h}{\frac{1}{2}\rho_\infty V_\infty^2 b_s c} \tag{21}$$

In the prior fixed wing circulation control studies, the change in lift coefficient of the airfoil was found to be dependent on the ratio of velocities; jet and freestream, V_j and V_∞. Eq. (22) is an empirical fit created by Loth and Boasson [16] to describe the circulation control lift enhancement. Combining Eq. (21) and Eq. (23) yields a relationship of the change in lift coefficient, as a function of the blowing coefficient, slot height, and chord length.

$$\Delta C_L = 40\left(\frac{h}{c}\right)^{0.64}\left(\frac{V_j}{V_\infty} - 1\right) \tag{22}$$

$$\Delta C_L = 40\left[\left(\frac{h}{c}\right)^{0.14}\sqrt{\frac{\rho_\infty C_\mu}{2\rho_j}} - \left(\frac{h}{c}\right)^{0.64}\right] \tag{23}$$

4. AERODYNAMIC PERFORMANCE MODIFICATIONS

Circulation control was initially considered such that the open blowing slots near the trailing edge of the airfoil are in the direction of the lift force. In other words, when the airfoil is at positive angles-of-attack, the blowing slot on the upper surface of the airfoil will be opened, and at negative angles-of-attack the lower surface blowing slot is opened. In order to simulate this transition the data from 0 to 180 degrees was inverted and applied from 0 to -180 degrees as shown in **FIGURE 6** for the lift coefficient and **FIGURE 7** for the drag coefficient.

The lift and drag coefficient plots in **FIGURE 6** and **FIGURE 7** were based on the data presented by Pawsey [6] as the non-circulation controlled performance. Circulation control enhancement of the lift, as described by Loth and Boasson [16] in Eq. 21, and the corresponding increase in induced drag, was applied at angles of attack ranging from -15 to 15 degrees, which is the only region where circulation control blowing is currently applied in these idealized lift and drag curves. In this range, a considerable increase in lift coefficient can be achieved which can in turn be utilized to enhance the performance of the wind turbine. The increased enhancement will be most beneficial during low tip speed ratio operation, which provides a wider range of useful wind speeds.

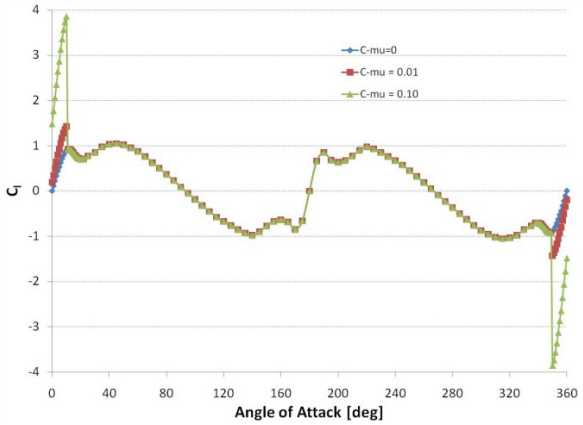

FIGURE 6: Lift Coefficient Determined for the Blowing Coefficients of 0, 0.01, and 0.10.

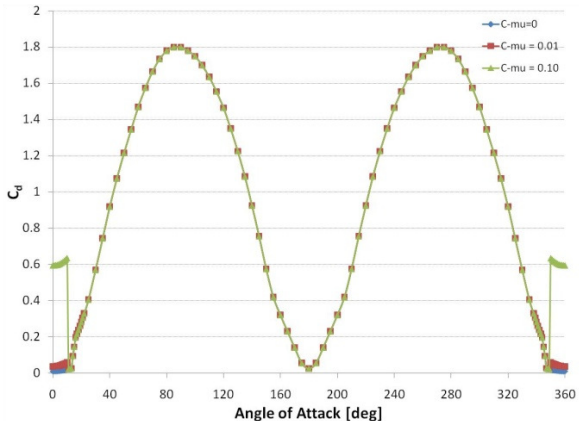

FIGURE 7: Drag Coefficient Determined for the Blowing Coefficients of 0, 0.01, and 0.10.

Since the application of circulation control requires a modification to the trailing edge of the airfoil, and existing literature has no general theory for the precise prediction of the augmented aerodynamic forces for this application, an experiment was undertaken to expand the understanding of parameters which influence the performance of circulation control. A model was developed based on the NACA 0018 airfoil with a 9 inch chord-length. The airfoil model was modified by creating a rounded trailing edge, with ~0.015 inch blowing slots located at the vertical apex of the cylindrical trailing edge. This modification resulted in a physical chord length of 8 inches and a thickness ratio of 20.3% for the test model and is shown in **FIGURE 8**, as installed in the West Virginia University Closed Loop Wind Tunnel. This test specimen was tested at a variety of air speeds and over the required range of angles of attack. The results obtained were in the form of lift and drag coefficient curves.

FIGURE 8: Experimental Set-up of the Modified NACA 0018 Airfoil Model, as Tested in the WVU Closed Loop Wind Tunnel

5. RESULTS AND CONCLUSIONS

The lift and drag curves resulting from the experiments are shown in FIGURE 9 and **FIGURE 10**, respectively, are the key results of the tests on the modified NACA 0018 airfoil. These results indicate an increase in the lift coefficient, at zero degrees for the non-blown C_l = 0, and for blowing at a C_μ = 0.10 resulted in a lift coefficient of approximately 1; and as expected the drag was also found to increase. These lift augmentation curves are approximately one half the values documented by previous investigations Englar [11], Gibbs [15], and Harness [17]. The limited performance of the circulation control in the current research was attributed to the smaller trailing edge radius incorporated into the NACA 0018 Circulation Control model. This decrease in lift augmentation potential was deemed acceptable due to the penalties associated with large profile drag of a large diameter trailing edge. This trade-off will be considered in future work.

FIGURE 11, shows the vortex model predictions with the various blowing coefficients against the inverse of the tip speed ratio, which reveals that the blowing coefficient has a similar influence on the performance of the wind turbine as the various potential solidity factors, compared to FIGURE 4 in that the shape of the curve is slightly modified in width and location of the peak. The benefit of using circulation control is that the blades' performance can be changed on the fly during operation of the wind turbine, which is not possible with a non-augmented blade. A computerized system can be incorporated to customize the circulation control blowing coefficient to maximize the performance over a wide range of tip speed ratios. In lieu of using the site specific wind conditions needed to estimate the annual energy gain, the area under the C_p-λ curve can be used to represent the comparative difference in the annual energy production independent of the site specific wind conditions. The area under the "*Base"* curve was found to be 0.0423 and the *"Variable* σ*"* curve was found to be 0.0654. Allowing the circulation control augmented wind turbine to effectively capture energy at the peak performance coefficient over a range of blowing conditions, yields approximately a 50% increase in the area under the performance curve. It is important to note that this is an idealized measure of the performance over a range of wind speeds and may not reflex the gains in total power generated in the actual wind conditions and have yet to account for the power required to supply the blown air and other performance factors

of the circulation control. Some of these factors include the maximum blowing coefficient, the tip speed ratio when circulation control is phased out, as well as the duration of the blowing.

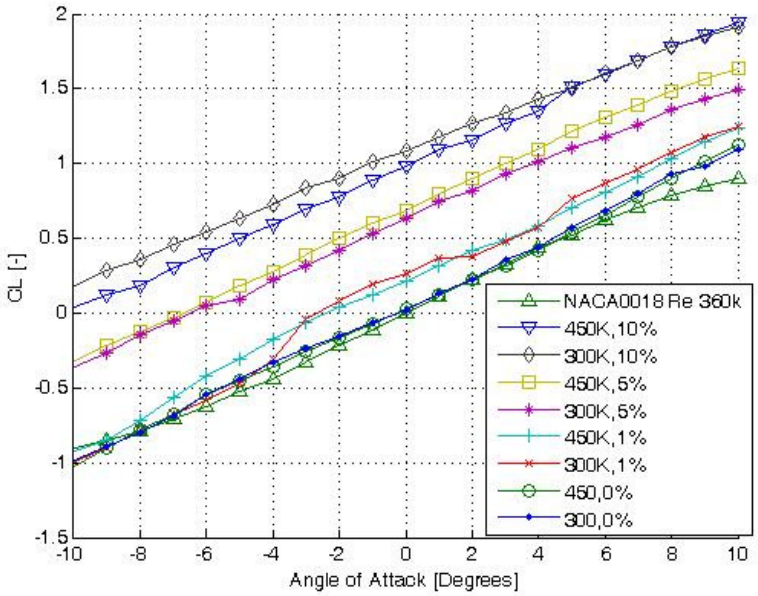

FIGURE 9: Experimentally Determined Lift Coefficient Curves for the Circulation Control Augmented NACA 0018.

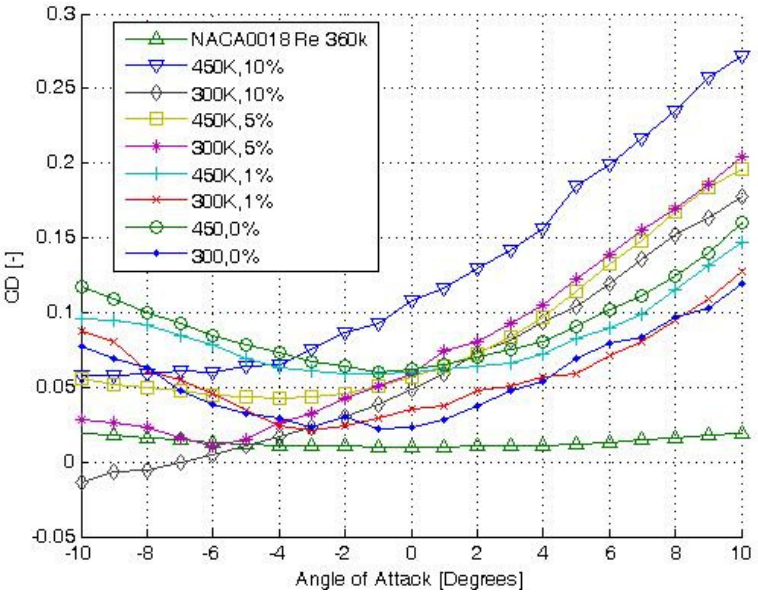

FIGURE 10: Experimentally Determined Drag Coefficient Curves for the Circulation Control Augmented NACA 0018.

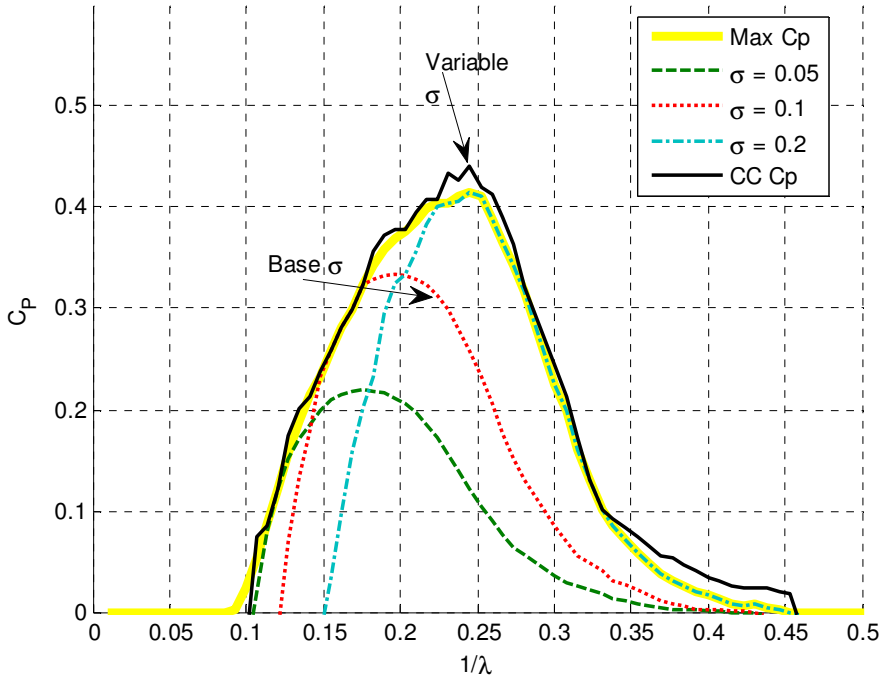

FIGURE 11: Estimated Performance for Solidity Factor of 0.1 with Blowing for the Investigated Blowing Coefficients, Wilhelm [18].

From the projected performance of the circulation control augmented vertical axis wind turbine, FIGURE 11, the regions of the world upon which large wind turbines can be installed can be increased. Large wind turbines, generally referred to as "Utility Size", tend to operate at a fixed rotational speed and are directly connected to the electrical grid. Consequently, as the wind speed varies the tip speed ratio also varies, resulting in a change in the coefficient of performance. The adaptation of circulation control to the wind turbine has been simulated and yields a potential method to alter the performance curve of the wind turbine to tailor the performance to the current wind conditions of the site. In consistent wind environments this adaptation provides less benefit. However, in environments with predominant wind at a variety of speeds the use of circulation control can potentially enhance the turbine performance by 5% to 50%. The amount of improvement due to circulation control depends on the engineering trade-offs of the maximum blowing coefficient, tip speed ratio at which blowing is phased out, wind distribution, height of the blown jet, duration of the blowing (% of the blades path), and the span of the blowing jet (% of the turbine rotor height).

These results lead to the conclusion that circulation control has a potential impact on the future of wind turbines, particularly VAWT's, and should be further evaluated by experimental means, particularly methods to enhance the jets interaction with the flow such as ejectors or injectors near the jet. Another issue which needs further examination is the power required to provide the compressed air to the blowing slots. The estimated power can be experimentally determined for the various blowing coefficients and used to develop the upper and lower limits of when to apply the circulation control and how to manipulate the flow rate to maximize the energy capture while minimizing the power required and making the concept cost effective.

6. NOMENCLATURE

Symbol	Meaning
A	Turbine Rotor Area
A_{shaft}	Internal Ducting Area of Shaft
b_j	Span of Jet
b_s	Span of Turbine Blade

c	Chord Length of Blade
C_l	Lift Force Coefficient
C_n	Normal Force Coefficient
C_p	Coefficient of Performance
$C_{P_{element}}$	Coefficient of Performance per Element Span
C_t	Tangential Force Coefficient
C_μ	Blowing Coefficient
$d\ell$	Incremental Length
F_n'	Normal Force per Unit Span
F_n^+	Non-Dimensional Normal Force per Unit Span
F_t'	Tangential Force per Unit Span
F_t^+	Non-Dimensional Tangential Force per Unit Span
h	Height of the Blowing Slot
HAWT	Horizontal Axis Wind Turbine
h_c	Radial Height of a Vortex
L'	Lift per Unit Span
P	Power
P_{max}	Maximum Power
P_η	Power Incorporating Compressor Efficiency
r	Radial Location
R	Turbine Radius
S	Blade Area
T_e^+	Non-Dimensional Torque per Blade Element
U_R	Resultant Velocity
U_T	Tangential Velocity
V_1	Upstream Wind Speed
V_2	Downstream Wind Speed
VAWT	Vertical Axis Wind Turbine
V_c	Velocity at Edge of Vortex Core
V_j	Jet Velocity
V_∞	Wind Speed
ΔC_l	Change in Lift Coefficient Due to Circulation Control
Δt	Time Step
$\Delta\theta$	Angular Step
η	Compressor Efficiency
Γ	Circulation
Γ_B	Bound Circulation
Γ_s	Shed Circulation
λ	Tip Speed Ratio
ρ	Density
σ	Solidity Factor
ω	Rotational Speed of Turbine

7. REFERENCES

[1] Georges Jean Marie Darrieus, "Turbine Having Its Rotating Shaft Transverse to the Flow of the Current," 1,835.018, December 1931.

[2] K.A. Kuhlke, "An Experimental Investigation of the WVU Straight Bladed Darrieus Wind Turbine," Morgantown, WV, MS Thesis 1978.

[3] P.G. Migliore, "A Free-Vortex Model with Numerical Solution for the Unstead Lifting Characteristics of Straight Bladed Darrieus Wind Turbines," Morgantown, WV, Ph.D.

Dissertation 1978.

[4] P. G. Migliore, W. P. Wolfe, and R. E. Walters, "Aerodynamic Tests of Darrieus Turbine Blades," 1980.

[5] J. H. Strickland, B. T. Webster, and T. Nguyen, "A Vortex Model of the Darrieus Turbine: An Analytical and Experimental Study," Alburquerque, NM, 1980.

[6] N.C.K. Pawsey, *Development and Evaluation of Passive Variable-Pitch Vertical Axis Wind Turbines. Diss.* New South Wales: University of New South Wales, 2002.

[7] David McGrain, Gerald M Angle II, Jay P Wilhelm, Emily D Pertl, and James E Smith, "Circulation Control Applied to Wind Turbines," , San Francisco, CA, USA, 2009.

[8] B.G. Newman, "The Deflexion of Plane Jets by Adjacent Boundaries - Coanda Effect," in *Boundary Layer and Flow Control, Vol. 1.*: Pergamon Press, 1961, p. 232.

[9] R. A. Churchill, "Coanda Jet Around a Cylinder with an Interacting Adjacent Surface," Morgantown, WV, Ph.D. Dissertation 1992.

[10] J. P. Ambrosiani, "Analysis of a Circulation Controlled Elliptical Airfoil," Morgantown, WV, Ph.D. Dissertation 1971.

[11] R.J. Englar, "Two-Dimensional Subsonic Wind Tunnel Tests of Two 15-Percent Thick Circulation Control Airfoils," Tech. Note AL-211 1971.

[12] R. J. Kind, "A Calculation Method for Circulation Control by Tangential Blowing Around a Bluff Trailing Edge," *Aeronautical Quarterly*, p. Vol. XIX, 1968.

[13] R J Kind and D J Maull, "An Experimental Investigation of a Low-Speed Circulation-Controlled Aerofoil," *Aeronautical Quarterly Vol. XIX*, pp. 170-182, May 1968.

[14] Danny P. Myer, "An Experimental Investigation of a Circulation Controlled Cambered Elliptical Airfoil with a Rounded Trailing Edge," Morgantown, WV, MS Thesis 1972.

[15] E.H. Gibbs, "Analysis of Circulation Controlled Airfoils," Morgantown, WV, Ph.D. Dissertation 1975.

[16] J. L. Loth and M. Boasson, "Circulation Contol STOL Wing Optimization," *Journal of Aircraft*, pp. Vol. 21 No. 2 pp. 128-134, 1983.

[17] Gregory S. Harness, "An Experimental Investigation of a Circulation Controlled Cambered Elliptical Airfoil," Morgantown, WV, MS. Thesis 1970.

[18] Jay P. Wilhelm, "Power Envelope Expansion using a Solidity Matching Scheme for a Circulation Controlled Vertical Axis Wind Turbine," Morgantown, WV, PhD Dissertation 2010.

[19] C. Trevelyan, "Application of Circulation Control Aerofoils to Wind Turbines," Leicestershire, UK, Ph.D. Dissertation 2002.